The ω-Phase as an Example of an Unusual Shear Transformation

J. C. WILLIAMS, D. de FONTAINE, AND N. E. PATON

The conditions leading to formation of the metastable ω-phase in Ti, Zr, and Hf alloys are described and earlier experimental observations directly related to ω-phase formation are summarized. New experimental results are presented which show that increased oxygen content suppresses athermal ω-phase formation in Ti-V alloys. A mechanism of ω-phase formation based on the formation of a linear displacement defect is described and it is shown that both the earlier and new experimental results are consistent with this mechanism. Additional experimental results on variations in electrical and physical properties in Ti alloys are also shown to be consistent with the linear displacement defect model.

THE ω-phase is a metastable decomposition product which forms in bcc (β-phase) alloys based on Ti, Zr, and Hf which have been partially stabilized by suitable alloying additions. Occurrence of the phase was first encountered by Frost, *et al.*[1] who found that aged Ti-Cr alloys containing ~8 wt pct Cr were unexpectedly brittle. Subsequent X-ray diffraction patterns obtained from these alloys showed that a second phase was present which was designated the ω-phase. Since these early experiments of Frost, *et al.*, the ω-phase has received extensive study, initially because of its deleterious effects on mechanical properties, later because of its influence on such physical properties as superconductivity and most recently because the $\beta \rightarrow \omega$ transformation exemplifies an interesting class of phase transformations.

In this paper we will attempt to recount briefly the pertinent background information with regard to the various aspects of ω formation, including the remaining unresolved issues; we will then present some recent experimental results, together with our views regarding the transformation and show how these views help unify the subject.

BACKGROUND

It is well-known that the ω-phase can be formed in metastable bcc alloys of Ti, Zr, and Hf during quenching (athermal ω) or during aging (isothermal ω); further, these two forms of ω-phase have been separated in many earlier treatments of the subject.[2-4] Such separation has largely been based on observed variations in intensity and breadth of the ω-phase X-ray diffraction lines leading to the term "diffuse ω" for athermal ω. As will be demonstrated below, no physical basis exists to justify such a separation. Thus, in the following portions of this paper the terms athermal and isothermal will only be used to describe the thermal conditions whereby the ω under discussion has been formed.

The composition range over which athermal ω-phase forms has been shown to depend on the type of solute and, according to some investigators,[5,6] on the electron-atom ratio of the alloy which is controlled by the solute valence and concentration. The justification for the latter point is not clear since several schemes have been employed to assign valence to transition element solutes and all seem to produce a correlation. Furthermore, the solute-rich composition limit for athermal ω-phase formation has been subject to disagreement; the bulk of these disagreements are largely traceable to the relative detectability of athermal ω by various experimental techniques. For example, early workers usually employed variations in hardness to indicate the presence of athermal ω-phase. Recent studies have shown that little or no hardening accompanies ω formation until the vol fraction exceeds 0.2 to 0.25;[7] thus the use of hardness measurements introduces a significant underestimate of the composition limit for athermal ω formation. X-ray diffraction has probably been the most successful technique for ω detection although many recent studies have employed selected area electron diffraction for this purpose. Comparison of the electron and X-ray diffraction results have been complicated by two factors. Firstly, the detection of small vol fractions of ω can only be reliably accomplished using single crystal X-ray techniques, such techniques have not gained wide acceptance due to the relative scarcity of single crystals. Secondly, the electron diffraction patterns contain complex networks of diffuse intensity, the nature of which will be described below.[8,9] The diffuse intensity overlaps the ω diffraction maxima positions, causing the detection of ω in such patterns to become somewhat subjective. Thus, while the $\beta \rightarrow \omega$ transformation in principle occurs at a well-defined temperature (ω_s) for a given concentration, in practice the experimental difficulties enumerated above have caused the solute rich composition limit to be ill-defined.

In addition to the above experimental difficulties, it has recently been shown by Paton and Williams[10] that minor alloying element concentration can have a large effect on ω_s. They found that the amount of oxygen in a series of Ti-V alloys could change ω_s by more than 100°C over a range of oxygen commonly encountered

J. C. WILLIAMS, Group Leader, and N. E. PATON, are with the Physical Metallurgy and Materials Group, Science Center, Rockwell International, Thousand Oaks, Calif. 91360. D. de FONTAINE is Professor, Department of Materials Science, University of California at Los Angeles, Los Angeles, Calif. This paper is based on a presentation made at a symposium on "Phase Transformations in Less Common Metals: A Dialogue," held at the Fall Meeting in Cleveland on October 16, 1972, under the sponsorship of the Phase Transformations Activity, Materials Science Division, American Society for Metals.

in laboratory heats. These results are shown in Fig. 1. Much of the disagreement over the composition dependence of ω_s may thus be attributed to variations in concentration of minor alloying elements such as interstitial O. This effect of interstitials on ω_s may also have important implications in terms of the transformation itself, as discussed later.

The diffuse streaking in electron diffraction patterns has been reported in a wide variety of bcc Ti, Zr, and Hf base alloys. This streaking, which roughly can be described as sheets of intensity lying on (111) rel-planes, is illustrated in Fig. 2. As either the temperature or the solute concentration increases, the streaks become more curved (Fig. 3). The origin of this streaking has been analyzed in a previous article and this analysis will be described and elaborated in a later section of this paper.

In alloys which exhibit well-defined athermal ω intensity maxima, the phase has been shown to occur as 20 to 40Å diam particles of roughly equiaxed morphology. Sass[11] has reported that the particles often form in rows, however the generality of this effect is not clear at present.

Recent cooling stage experiments performed in the electron microscope have also demonstrated that ω can form athermally at temperatures as low as 90 K;[12] these experiments have also demonstrated the total reversibility of the athermal $\beta \rightleftharpoons \omega$ transformation. Earlier Russian work[13] showed that extremely fast quench rates as high as 11,000°C per s were insufficient to suppress the athermal formation of ω. The combined observation of very rapid kinetics and low temperature transformation lead to an earlier suggestion that ω formed martensitically;[14] however the product phase does not conform to the requirements of a classical martensitic product. It has been suggested recently that $\beta \rightleftharpoons \omega$ transformation occurs by correlated displacements;[15] the details of this latter treatment will be described in a subsequent section since they comprise the central theme of this paper.

The structure of athermal ω-phase has been the subject of an earlier dispute between Silcock,[16] who claimed it belonged to space group D^1_{6H} ($P6/mmm$) and Bagariatskii[17] who claimed it belonged to D^3_{3D} ($P\bar{3}m1$). Recently Sass and Borie[18] have shown that increasing solute concentration causes the sixfold symmetry charac-

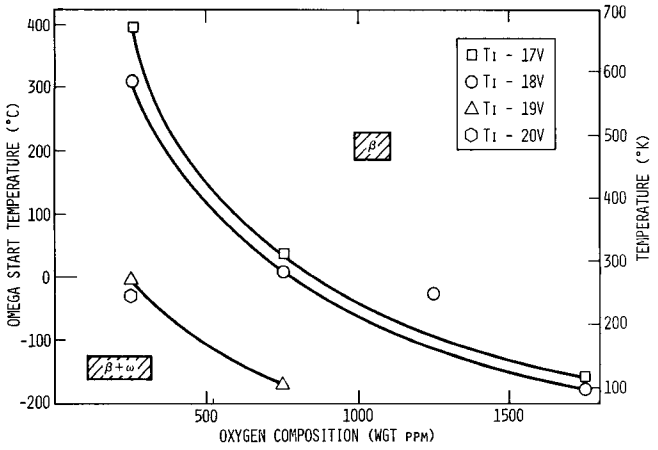

Fig. 1—Omega start temperature (ω_s) plotted vs oxygen composition for a series of Ti-V alloys.

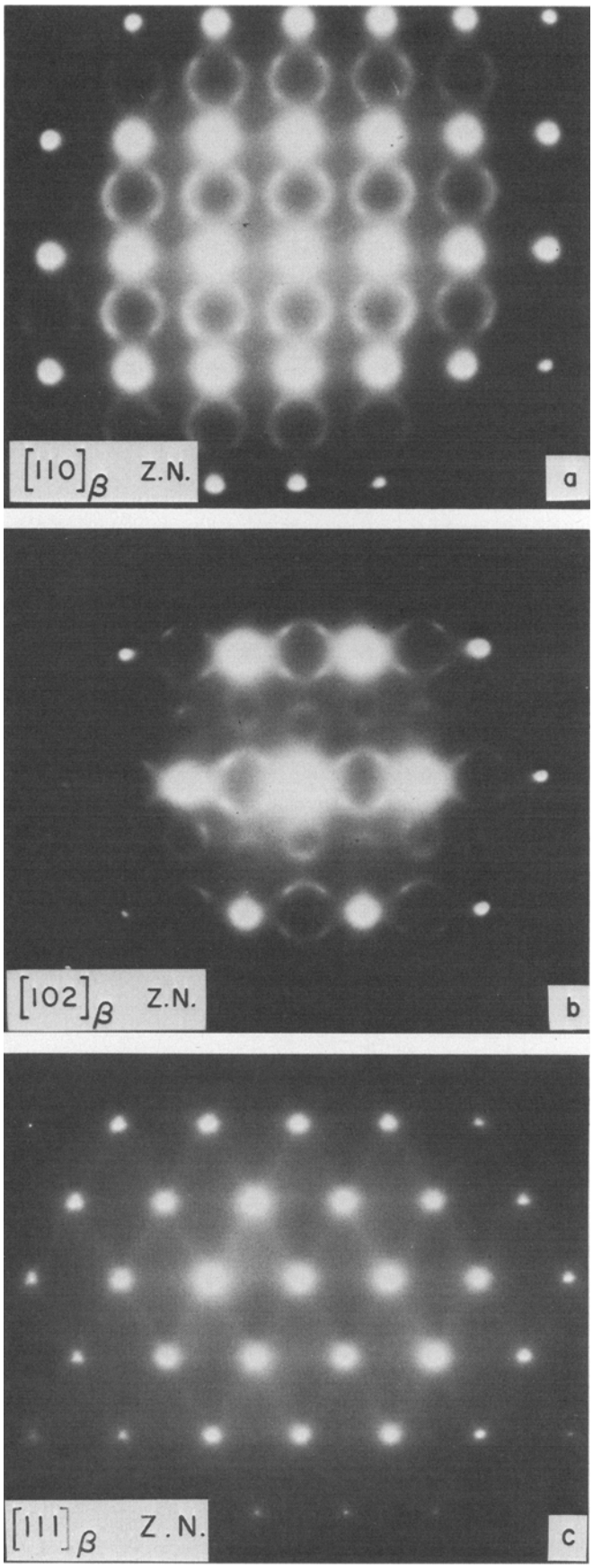

Fig. 2—Selected area diffraction patterns of a Ti-12 wt pct Fe alloy illustrating (111) rel-plane streaking. (*a*) [110]β zone normal, (*b*) [102]β zone normal, (*c*) [111]β zone normal.

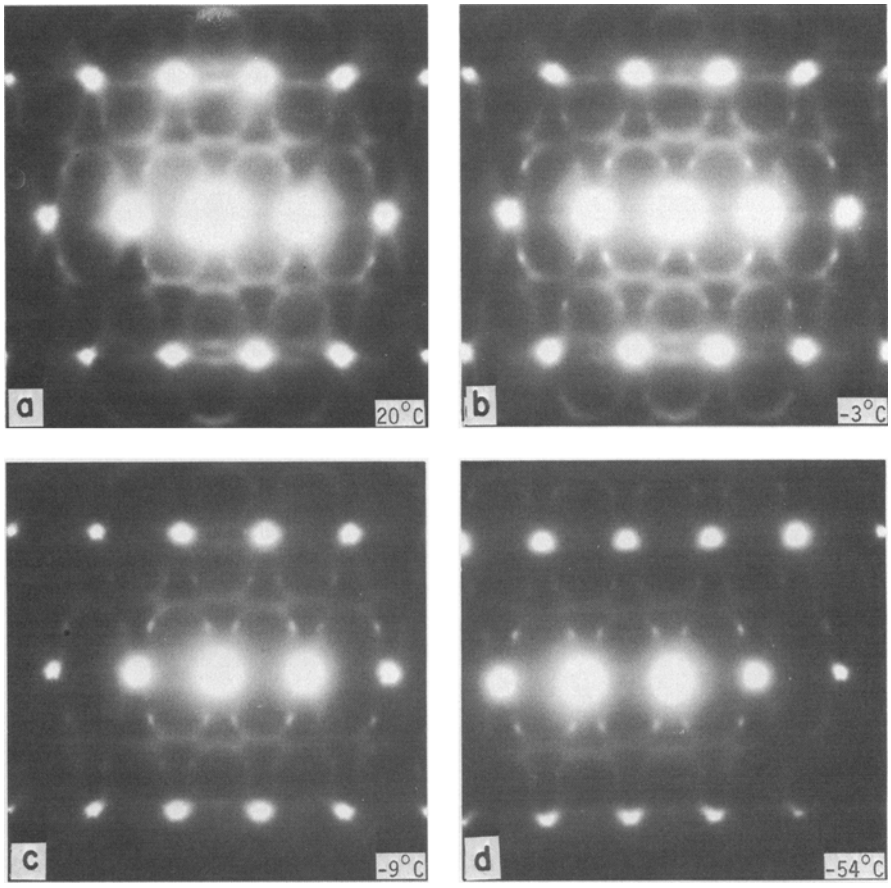

Fig. 3—Selected area diffraction patterns of a Ti-12 wt pct Mo alloy over a range of temperatures showing the increased curvature of the streaks as temperature increases.

teristic of D^1_{6H} to degenerate into the threefold symmetry characteristic of D^3_{3D}. Thus, it has been concluded that the differences in space group reported by Silcock and Bagariatskii stem from the particular alloy compositions each investigator studied. Silcock has also examined the structure of ω-phase in aged Ti alloys and reported it as D^1_{6H} (P6/mmm).

The isothermal ω-phase has two distinct morphologies; cuboidal and ellipsoidal[19] (Fig. 4). Hickman[20] has shown that the vol fraction of ω-phase increases rapidly during aging and stabilizes before compositional changes are complete. He also has shown that the isothermally formed ω-phase rejects solute during formation; the ω and β-phases reach metastable equilibrium compositions, leading to a varying misfit between the ω and the matrix. The prevailing morphology is determined by the misfit between the β-phase matrix and the ω-phase which in turn is controlled by the variations in β-phase lattice parameter with the particular solute type in question. This point has been convincingly demonstrated in Ti-V-Zr alloys where the misfit has been adjusted by ternary additions of Zr.[21] The kinetics of isothermal ω-phase formation are extremely rapid, even in solute-rich alloys which do not contain preexisting athermal ω-phase. For example, the vol fraction ω can reach 0.7 in a Ti-25 pct V alloy aged 10 min at 350°C.[20]

TRANSFORMATION MECHANISM

A crystallographic and atomistic description of the β to ω transformation is useful in order to obtain a picture of the ω structure, and is a necessary part of understanding the transformation mechanism itself. In discussing the transformation of the bcc β-phase to the hexagonal ω-phase, let us first neglect compositional effects and consider all atoms in a bcc Ti, Zr, or Hf-based solid solution as undifferentiated. This point of view is adequate for the description of the athermal ω transformation, as this transformation is not diffusion controlled and no composition changes are involved. As first suggested by Hatt and Roberts[22] and later developed by de Fontaine,[23] athermal $\beta \rightleftharpoons \omega$ transformation can be accomplished formally by collapsing a pair of neighboring (111) planes to the intermediate position, leaving the next plane unaltered, collapsing the next pair and so on. This operation produces a structure of hexagonal symmetry which, in the limit of complete double plane collapse, will be called the "ideal ω structure" which corresponds to the structure reported by Silcock as described above. A schematic representation of the formal mechanism of the β to ω transformation is shown in Fig. 5 where (111) planes are shown on edge. Note that submitting the lattice to a $\frac{2}{3}[111]$ longitudinal displacement wave of proper amplitude and phase produces the required transformation. This viewpoint has led to the interpretation of internal friction peaks found in Ti-V alloys in terms of an interaction between an external stress field and the [111] longitudinal displacement waves.[24]

An atomistic description of the β to ω transformation is given in Fig. 6. As in Fig. 5, Fig. 6(*b*) shows (111) lattice planes on edge. The bcc stacking sequence *ABCABC*··· is indicated. The projected bcc structure

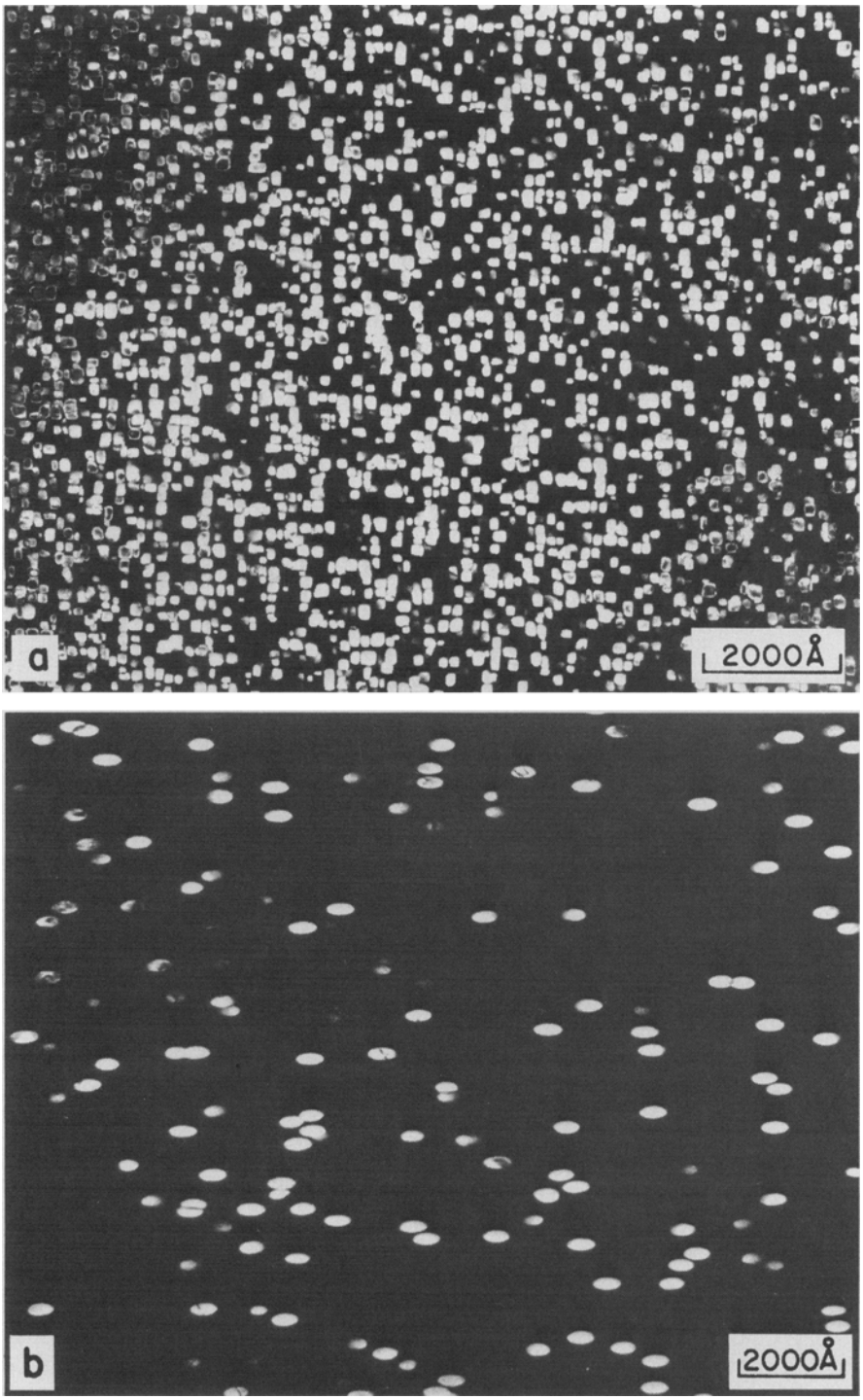

Fig. 4—Isothermal omega phase morphology. (*a*) Cuboidal in a Ti-8 wt pct Fe alloy, solution treated 900°C, 30 min and aged 400°C, 4 h. (*b*) Ellipsoidal in a Ti-11.5 wt pct Mo-5.5 wt pct Zr-4.5 wt pct Sn alloy (β-III), solution treated 900°C, 30 min and aged 480°C, 5 min.

is shown on the left (Fig. 6(*a*)) symbols ○ representing atoms in the plane of the figure, (+) above, and (−) below the plane. Upon double plane collapse, the ω structure is formed and the resulting structure, projected on (111) planes, is shown on the right (Fig. 6(*c*)). The stacking sequence is now $AB'AB'\cdots$, with filled circles representing atoms in the collapsed B' plane. According to this atomistic (rather than planar) description, the β to ω transformation can be accomplished formally by allowing all atoms in the (+) plane, say, to move by $\frac{1}{3}$ the nearest neighbor distance along each corresponding [111] close-packed row. This operation changes the (+) symbols of Fig. 6(*a*) to (−) symbols,

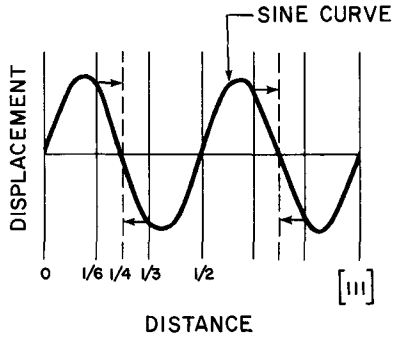

Fig. 5—Schematic representation of the mechanism of the β-ω transformation showing (111) planes on edge.

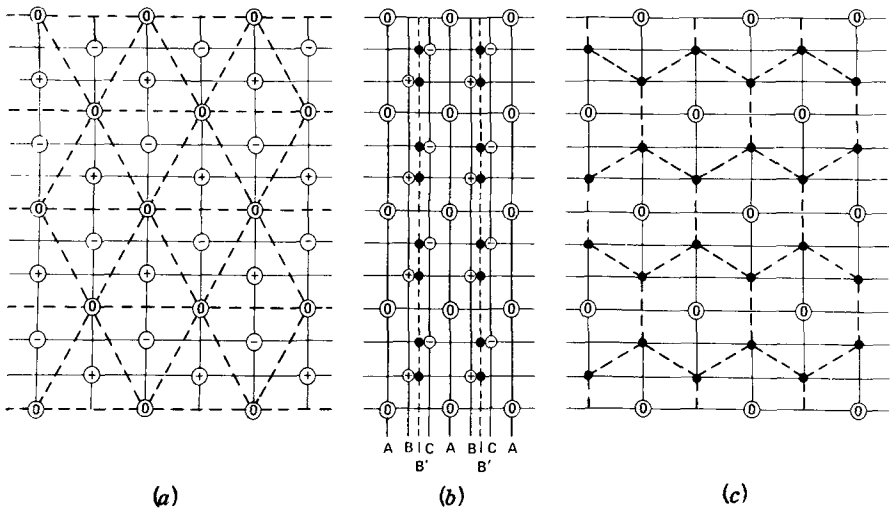

Fig. 6—Atomistic representation of the β-ω transformation. (*a*) bcc structure projected on (111) plane, (O) atoms in the plane of the figure, (+) above, and (−) below the plane. (*b*) (111) planes on edge showing bcc stacking sequence *ABCABC*. (*c*) (111) plane projection after double plane collapse to give ω structure with stacking sequence now *AB'AB'*, filled circles representing the *B'* plane.

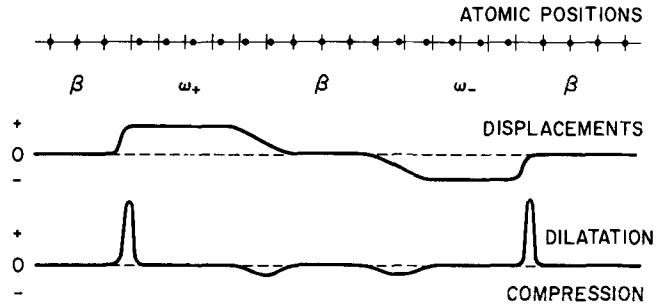

Fig. 7—Schematic representation of the linear defect showing displaced row segments.

making projection 6(*a*) resemble projection 6(*c*). The (−) plane is now the collapsed one. Relaxation will, of course, occur so that the double (−) plane will take up the intermediate *B'* position. Note the change of threefold symmetry around the [111] direction in the β structure, to sixfold symmetry in the ideal ω structure (Fig. 6(*c*)). If an atom is displaced along [111] by $\frac{1}{3}$ of the unit distance, it becomes captured in a neighboring (111) plane and establishes trigonal coordination in the plane of capture.

It is reasonable to assume that displacement of one atom along a nearest neighbor direction will induce like displacements of its neighbors along the atomic row, creating a displaced row segment or linear defect, a schematic representation of which is given in Fig. 7. Dots represent atomic positions, the vertical lines denoting the equilibrium β positions of the bcc lattice. The atomic positions at $+\frac{1}{3}$ and $-\frac{1}{3}$ of the nearest-neighbor distance are denoted ω_+ and ω_-, respectively. Row segments in ω positions are separated from row segments in β positions by transition regions of compression and dilatation, as indicated. These regions of dilatation and compression have prompted de Fontaine and Buck[15] to compare the linear defect to the vacancy and crowdion type defects postulated as a diffusion mechanism in other bcc metals and applied to the interpretation of radiation damage.

If partially covalent trigonal bonds are relatively favored in Ti, Zr, and Hf alloys, it is expected that linear defects of the type described will be prevalent over a wide range of temperatures, *i.e.*, longitudinal displacive correlations will exist up to relatively high temperatures. By contrast, interrow correlations should make their appearance at relatively low temperatures. Since the interrow correlations are two-dimensional, critical behavior is expected. The possible existence of a phase transition corresponding to the appropriate ordering of neighboring parallel linear defects was demonstrated elsewhere by Monte-Carlo simulation. The temperature at which long-range two-dimensional correlations set in is marked by the appearance, on diffraction patterns, of the extra ω reflections, as shown for example in the electron diffraction patterns of Fig. 8. The transition temperature is around 0°C in this example for Ti-15 wt pct Mo. A plausible real-space picture of the structure (relative to a single ⟨111⟩ variant) is offered by the Monte-Carlo computer simulation of a (111) projection of the alloy below the transition temperature, Fig. 9. This figure shows two interpenetrating conjugate ω domains, one consisting of minus symbols surrounding zeros, the other (with trigonal bonds outlined) consisting of zeros surrounding minuses. Two-dimensional order is, in this case, practically complete.

From the foregoing, it is possible to predict qualitatively the diffraction patterns expected at various temperatures. Above the ω transition, the linear defects belonging to a given ⟨111⟩ variant are uncorrelated and each displaced row thus diffracts practically independently of its neighbors. The diffuse intensity should therefore be concentrated in {111} rel-planes perpendicular to the variant in question. As two-dimensional correlations make their appearance in the vicinity of the ω transition temperature, the diffuse intensity must become modulated within the {111} rel-planes and must eventually peak at the $\frac{2}{3}$⟨111⟩ positions and other crystallographically equivalent points in reciprocal space. These effects are illustrated in Fig. 8. Recall that the $\frac{2}{3}$⟨111⟩ longitudinal displacement wave is precisely the one which formally converts the β to the ω structure. Thus, the two points of view, one of lattice displacement plane waves and one of two-dimensional correlations of linear defect are complementary: the local ordering of parallel row displacements creates an embryonic ω region which, in turn, can be regarded as a local $\frac{2}{3}$[111] static displacive mode.

Thus far, only a single ⟨111⟩ (or ω) variant was considered. Interactions between variants must also be

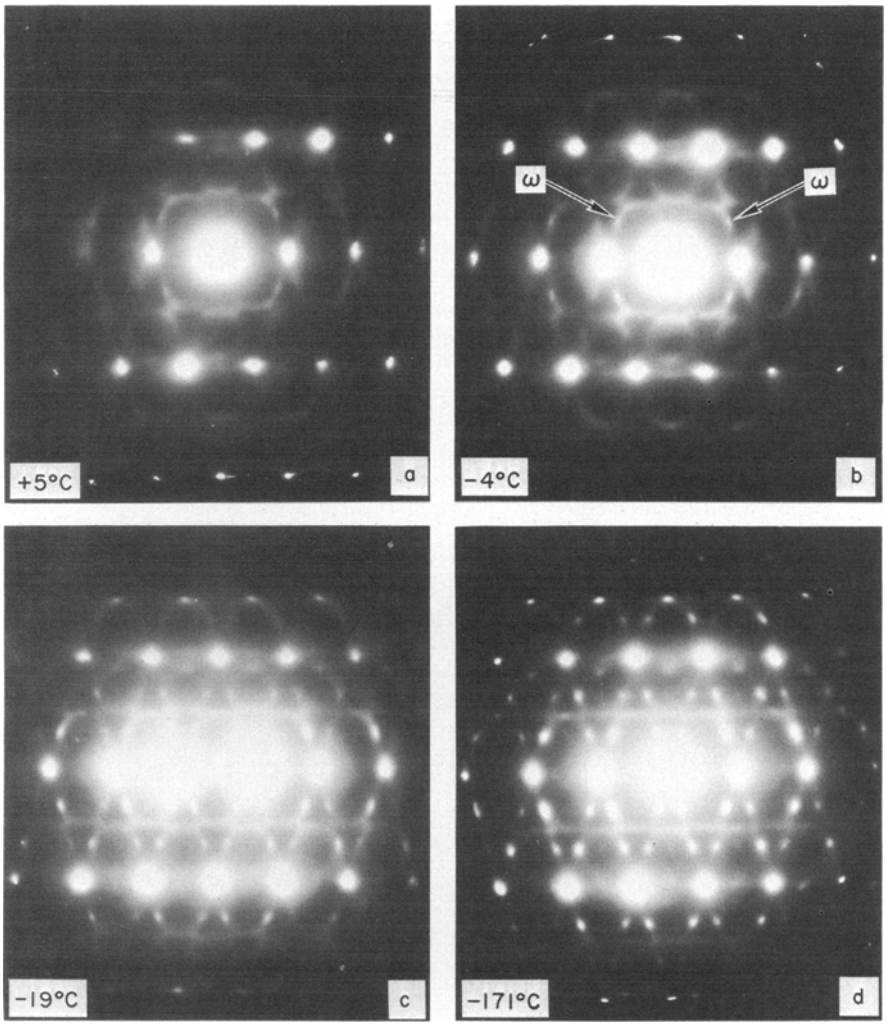

Fig. 8—Cooling series of a Ti-15 wt pct Mo alloy showing appearance of ω reflections (marked ω) at −4°C.

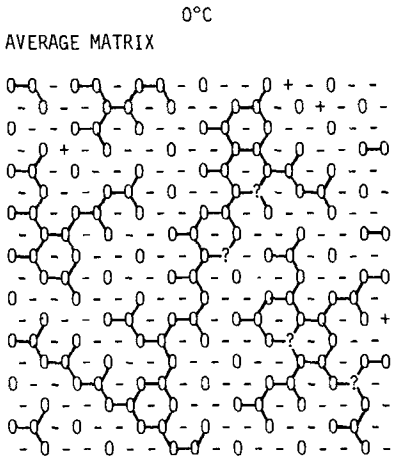

Fig. 9—Monte Carlo computer simulation of a (111) projection below ω_S, (○) atoms in the plane, (+) above, (−) below, and (?) in transition.

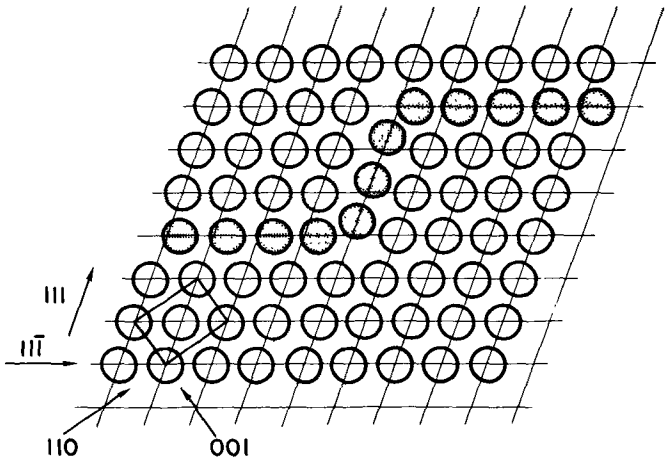

Fig. 10—Zig-zag defect resulting from interaction of linear displacement defects along intersecting [111] rows.

taken into account, however. For instance, a [11$\bar{1}$] displaced row segment will tend to produce a longitudinal displacement along an intersecting [111] row, which will induce further displacements along [11$\bar{1}$], and so forth. An example of the resulting zig-zag defect is illustrated in Fig. 10. Intervariant correlations have now been established so that, as shown in another connection by Cowley,[25] the diffuse intensity will tend to avoid the intersections of {111} rel-planes, just as a hyperbola avoids the intersection of its asymptotes. Thus, as was previously surmised, when intervariant interactions are significant, diffuse intensity will tend to depart from the octahedra formed by ⟨111⟩ rel-planes and lie, instead, in spheroids inscribed in the

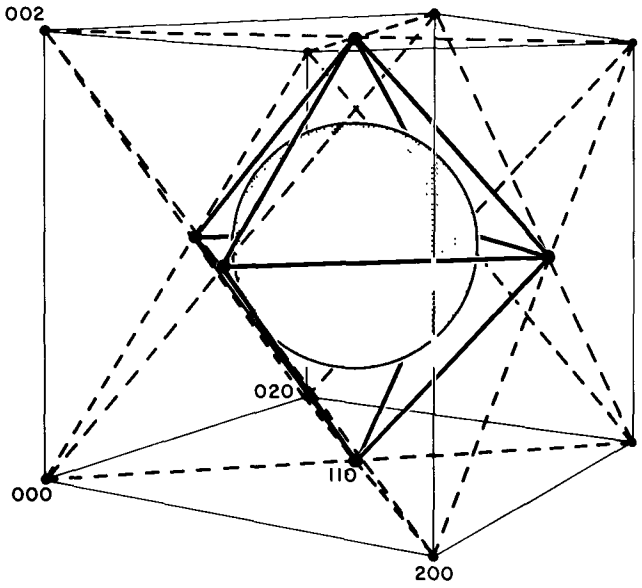

Fig. 11—Reciprocal space showing the sphere of diffuse intensity inscribed in the (111) rel-planes.

octahedra. One such resulting "sphere of intensity" is shown in Fig. 11. Corresponding diffraction patterns should then exhibit quasicircular streaking as shown for example, in Fig. 2.

Intervariant interactions are expected to be significant when ω domains are small. A highly distorted structure will then result; in such a case the double plane collapse of the ideal ω structure is not expected to go to completion. The resulting average structure will therefore exhibit threefold rather than sixfold symmetry, as discussed recently by Sass and Borie.[18]

There has been a tendency, in the metallurgical literature, to distinguish carefully between the athermal and the aged ω varieties. Actually, we believe that the basic mechanism of formation of these phases is unique. It can be shown, from qualitative free energy considerations, that direct conversion of β to ω without compositional changes can only lower the free energy of the alloy if the solute concentration is sufficiently lean (if it is too lean, a direct β to α martensitic reaction is favored). Thus, diffusionless β to ω transformation is thermodynamically favored only in a fairly narrow compositional range (as can be seen in Fig. 12). If, however, a metastable β solid solution of concentration somewhat beyond the athermal range is maintained for a sufficient length of time at temperatures for which diffusion rates are appreciable, favorable concentration fluctuations can occur in the β matrix creating solute-lean embryos of composition located within the athermal range, whereupon the embryos will transform spontaneously to ω by the athermal mechanism discussed above. Solute partitioning can then follow to conform to the phase boundaries of the metastable $\beta + \omega$ phase diagram.

DISCUSSION

The foregoing has attempted to describe the development of the current state of understanding of the $\beta \rightleftharpoons \omega$ transformation and then to present a model of the transformation which appears to account for the observed features of it. The model is additionally attractive because it provides a common basis for describing both

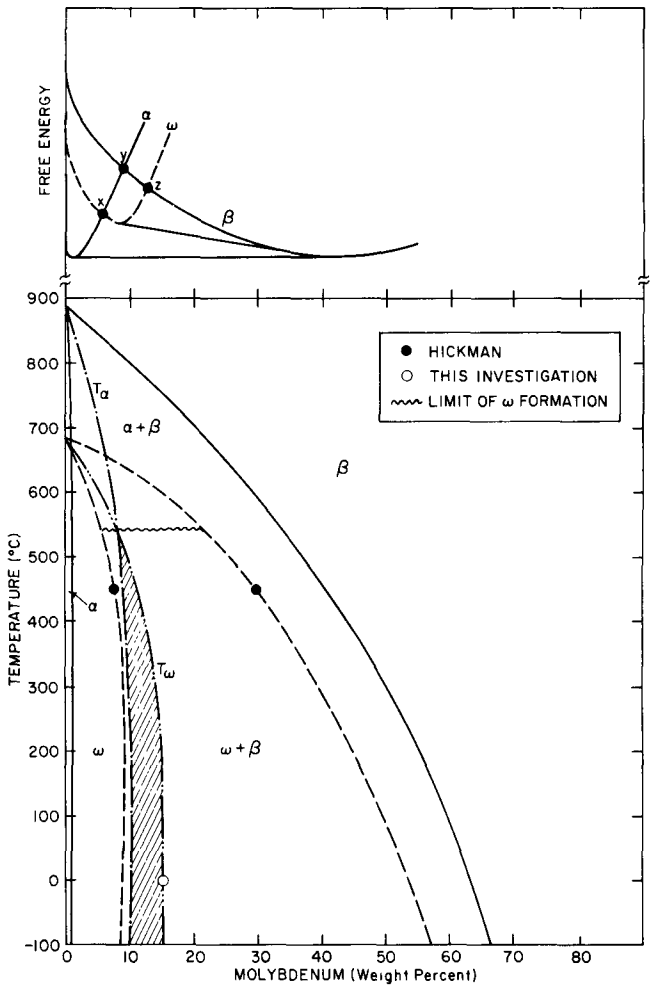

Fig. 12—Typical metastable phase diagram (from Ref. 3) illustrating the narrow composition range for athermal ω formation. $T\omega_S$ is the omega start temperature.

athermally and isothermally formed ω-phase. The following discussion is intended to amplify several features of the model and to reinterpret several earlier experimental observations in terms of it.

The damping peaks which are observed in bcc Ti and Zr alloys, in the alloy composition-temperature regime over which athermal ω forms, have been recently ascribed to the occurrence of stress induced atomic displacements[24] similar to those associated with the linear displacement defects described above. The temperature and frequency dependence of such damping peaks are consistent with thermally activated formation and/or migration of linear defects.[15] While the occurrence of a damping maximum does not elucidate the detailed nature of the defects, it is proof that the defects, whatever their nature, have an associated stress field which can interact with the applied oscillating stress. Further, Paton and Williams[26] have recently shown that oxygen in amounts up to ~2000 wt ppm significantly strengthens the β-phase. It is, therefore, reasonable to postulate that the stress fields of the linear defects and those of the interstitial oxygen atoms will interact. Accordingly, the observed effects of oxygen on ω_s can be accounted for since the interstitial oxygen is expected to interact with the linear defects, thereby pinning them at their extremities; such interactions will impede the ordering of neighboring linear defects required for occurrence of the $\beta \rightleftharpoons \omega$ transformation.

The trigonal coordination bonds which accompany the existence of linear displacement defects have been suggested to be partially covalent in nature. Formation of such bonds may be related to the anomalous negative temperature coefficient of electrical resistivity[27] reported in many metastable bcc Ti alloys since any tendency toward covalent bonding removes electrons from the conduction band. The increased density of covalent trigonal bonds with decreasing temperature is consistent with the increased resistivity, presumably because more electrons are involved in the trigonal bonding.

We have suggested that isothermal ω formation is preceded by a composition fluctuation which provides a solute-lean region which can subsequently transform to ω by the linear defect correlation mechanism. In this connection, Hickman[20] has shown that the isothermally formed ω does not immediately achieve metastable equilibrium composition, rather, the ω-phase vol fraction quickly stabilizes and the solute segregation occurs subsequently by diffusion. The rapid kinetics of isothermal ω formation coupled with the observation of lagging solute segregation suggests that the phase is easily nucleated and that subsequent growth is not diffusion controlled. We suggest that the long times required to achieve metastable equilibrium composition of the ω-phase are due to an increase in particle size after formation which is rapid compared to segregation and the attendant increase in diffusion distance. Thus, the characteristics of isothermal ω-formation more closely resembles athermal ω formation than those of a classical nucleation and growth reaction. Such characteristics also are consistent with the occurrence of a fluctuation as described above.

The sheets of diffuse intensity which lie on $\{111\}$ rel-planes have been reported in wide range of bcc alloys by several investigators.[11,21] Sass[8] has ascribed this diffuse intensity to the occurrence of ω-phase particles which are aligned in rows and has presented transmission electron microscopy evidence to support his point of view. However, in a later publication, Balcerzak and Sass[3] have reported the persistence of comparable diffuse streaking effects in Ti-Nb alloys containing up to 57 at. pct Nb, yet they were not able to image rows of ω-phase particles in alloys containing 34, 47, and 57 at. pct Nb. We suggest that the diffuse streaking may be due to the presence of linear displacement defects which can exist over the entire composition range. Since the linear defects lie along $\langle 111 \rangle_\beta$ they should produce a sheet of diffuse intensity normal to themselves or along $\{111\}$ rel-planes. This suggestion predicts diffraction effects consistent with the experimental observations, yet obviates the difficulty associated with a model which requires rows of ω particles since existence of such rows have not always been shown to accompany diffuse streaking.

Finally, it is useful to inquire about the generality of linear displacements along $\langle 111 \rangle$ in bcc metals other than Ti, Zr, and Hf alloys. In this connection it has been reported that the correlation of longitudinal atomic displacements along (111) rows appears to be a general feature of the bcc metals, evidenced by intense temperature defect scattering located in (111) reciprocal lattice planes.[28] Thus, the extension of large-amplitude longitudinal oscillations of close packed atomic row segments appears to be a direct consequence of geometry of the bcc lattice. In "normal" bcc metals row oscillations are about the equilibrium positions dictated by the bcc lattice, and this peculiar dilatational effect does not lead to static structural changes.

In the "anomalous" Ti, Zr, Hf metals and alloys there appears to be a second "metastable" position for the oscillating rows: namely, the "omega" position (see Fig. 7) which leads to trigonal bonding, as indicated in Figs. 6(*c*) and 9. It must, therefore, be concluded that this trigonal partial covalent structure is favored in the anomalous bcc, which is perhaps not surprising, considering that Ti, Zr, and Hf are group IV transition metals, that is, the metallic counterparts of C, Si, and Ge. Furthermore, it is surely no accident that the basal plane of the omega has the same honeycomb structure as the basal plane of graphite.

ACKNOWLEDGMENT

The authors wish to acknowledge the critical comments of Dr. Otto Buck.

REFERENCES

1. P. D Frost, W. M. Parris, L. L. Hirsch, J. R. Doig, and C. M. Schwartz: *Trans. ASM,* 1954, vol. 46, p 231.
2. J. M. Silcock, M. H. Davies, and H. K. Hardy. *The Mechanism of Phase Transformations in Metals,* p. 93, Institute of Metals Monograph, No. 18, 1955.
3. A. T. Balcerzak and S. L. Sass *Met. Trans.*, 1972, vol. 3, p 1601.
4. D. J. Cometto, G. L Houze, Jr., and R F. Hehemann: *Trans. TMS-AIME,* 1965, vol. 233, p. 30.
5. C. A. Luke, R. Taggart, and D H. Polonis *Trans. ASM,* 1964, vol. 57, p. 142.
6. B S. Hickman. *Trans. TMS-AIME,* 1969, vol 245, p. 1329.
7. J. C. Williams, B. S. Hickman, and H. L. Marcus. *Met. Trans.*, 1971, vol. 2, p. 1913.
8. S. L. Sass: *Acta Met.*, 1969, vol. 17, p. 813.
9. D. de Fontaine, N. E. Paton, and J. C. Williams. *Acta Met.*, 1971, vol. 19, p 1153
10. N. E. Paton and J. C. Williams *Scripta Met.*, 1973, vol. 7, p. 647.
11. S. L. Sass: *J. Less Common Metals,* 1972, vol 28, p. 157.
12. N. E. Paton, D. de Fontaine, and J. C. Williams: *Proc. 29th Annual Meeting of the Electron Microscopy Society of America,* p 122, Boston, Mass., 1971.
13. Y. A. Bagariatskii and G. I. Nosova *Fiz. Metal. Metalloved.*, 1962, vol. 13, p 415.
14. D. Stewart, B. A. Hatt, and J. A. Roberts *Brit. J. Appl. Phys.*, 1965, vol. 16, p. 1081.
15 D de Fontaine and O. Buck *Phil. Mag.*, 1973, vol. 27, p. 917.
16. J. M. Silcock *Acta Met.*, 1958, vol. 6, p. 481.
17. Y. A. Bagariatskii, T. V. Tagunova, and G. I. Nosova *Dokl. Akad. Nauk, SSSR,* 1955, vol 105, p. 1225.
18. S. L Sass and B. Borie ONR Tech. Report No 7, Project NR 031-734, January 1972.
19. M J. Blackburn and J C. Williams *Trans. TMS-AIME,* 1968, vol. 242, p. 2461.
20. B. S Hickman *J. Inst. Metals,* 1968, vol. 96, p 330.
21. J. C Williams, B. S Hickman, and D. H. Leslie *Met. Trans.*, 1971, vol. 2, p. 477.
22. B. A. Hatt and J. A Roberts *Acta Met*, 1960, vol. 8, p 575
23. D de Fontaine: *Acta Met.*, 1970, vol. 18, p. 275.
24. A. W. Sommer, S. Motokura, K. Ono, and O. Buck *Acta Met.*, 1973, vol. 21, p 489.
25. J. M. Cowley. *Acta Crystallogr.*, 1972, vol. A28, p. 5167.
26. N E. Paton and J. C. Williams Science Center, Rockwell International, Thousand Oaks, California, unpublished research, 1972
27. T. S. Luhman, R. Taggart, and D. H. Polonis· *Scr Met.*, 1968, vol 2, p 169.
28. G. Jonjo, S. Kodera, and H. Kitamura *J. Jap. Phys. Soc.*, 1964, vol. 19, p. 351.